Damage Produced in Model Solder (Sn-37Pb) Joints during Thermomechanical Cycling

X.W. LIU[1] and W.J. PLUMBRIDGE[1,2]

1.—Department of Materials Engineering, The Open University, Milton Keynes, United Kingdom.
2.—E-mail: W.Plumbridge@open.ac.uk

The microstructure of solder plays a key role in the reliability of electronic packages. In this study, the cyclic shear deformation experienced by Sn-37Pb solder joints was simulated by thermomechanically cycling model joints between 30°C and 125°C, and the nature of the damage investigated. Most of the developed shear strain was accommodated by the solder adjacent to the interface with the intermetallic layer, and its severity diminished exponentially with distance from the interface. Shear bands formed at this location and within the shear bands, significant microstructural coarsening occurred together with crack initiation on the outer free surface of the solder. Subsequent cycling produced multiple cracking, fragmentation, and macroscopic decohesion, progressing toward the interior of the solder. Secondary cracks initiated from the primary cracks and propagated along colony boundaries in the surface layers of the solder perpendicular to the shear direction. In the interior of the solder, well away from the interface with the intermetallic layer, a limited amount of coarsening occurred. Apart from smoothing of undulations, the intermetallic layer was unaffected.

Key words: Sn-Pb solder, model joint, thermomechanical cycling, microstructure

INTRODUCTION

A solder joint is an essential part of electronic devices, having a role not only for electrical and thermal conduction, but in surface-mount systems, also for mechanical support. Such interconnections are subjected to thermomechanical fatigue (TMF) throughout their service lives, and leadless surface-mount devices are particularly prone to this type of failure.[1–4] The primary cause is the strain developed because of the thermal-expansion mismatch between the chip carrier and the printed wiring board when the package experiences thermal fluctuations. The cyclic strains developed produce damage in the form of deformation, cracking, and eventual joint failure. An example of the development of these strains is shown schematically in Fig. 1a. The magnitude of the thermal shear strain, γ, depends upon the difference in thermal-expansion coefficients, the chip-carrier dimensions, and the thickness of the solder layer.

At room temperature, the homologous temperature, T_h, of the most common solder alloy, Sn-37Pb, is about 0.6, while extreme applications (temperature range of −55–130°C) represent values of T_h between 0.4 and 0.9. The combination of high homologous temperatures and cyclic straining can dramatically change the microstructure of the solder, producing coarsening, hardening/softening, grain-boundary sliding and separation, and cracking.[5–10] The role of intermetallic compounds and the interfacial structure that constitute the joint must also be considered.[11] It is inevitable that such changes will affect mechanical properties and the fatigue life of the solder joint. Reliable fatigue-life assessment of solder joints requires a good understanding of their microstructure and the changes induced by service conditions. Recent studies have examined the effect of prolonged isothermal aging on the microstructure of model butt joints between eutectic lead-tin solder and copper. Both phase coarsening and intermetallic thickening have been observed, and the kinetics and probable growth mechanisms identified.[12] Similar outcomes have been reported following temperature cycling of single solder ball, lap-shear specimens.[13] However, information relating to TMF under controlled and monitored conditions is limited.[14,15]

This study investigates microstructural evolution in Sn-37Pb model-solder joints that are uniformly shaped and subjected to thermomechanical cycling. Actual solder joints experience complex strains during service, but the primary strain is in shear.[16] Because of their size and shape, accurate quantification

(Received August 30, 2002; accepted January 2, 2003)

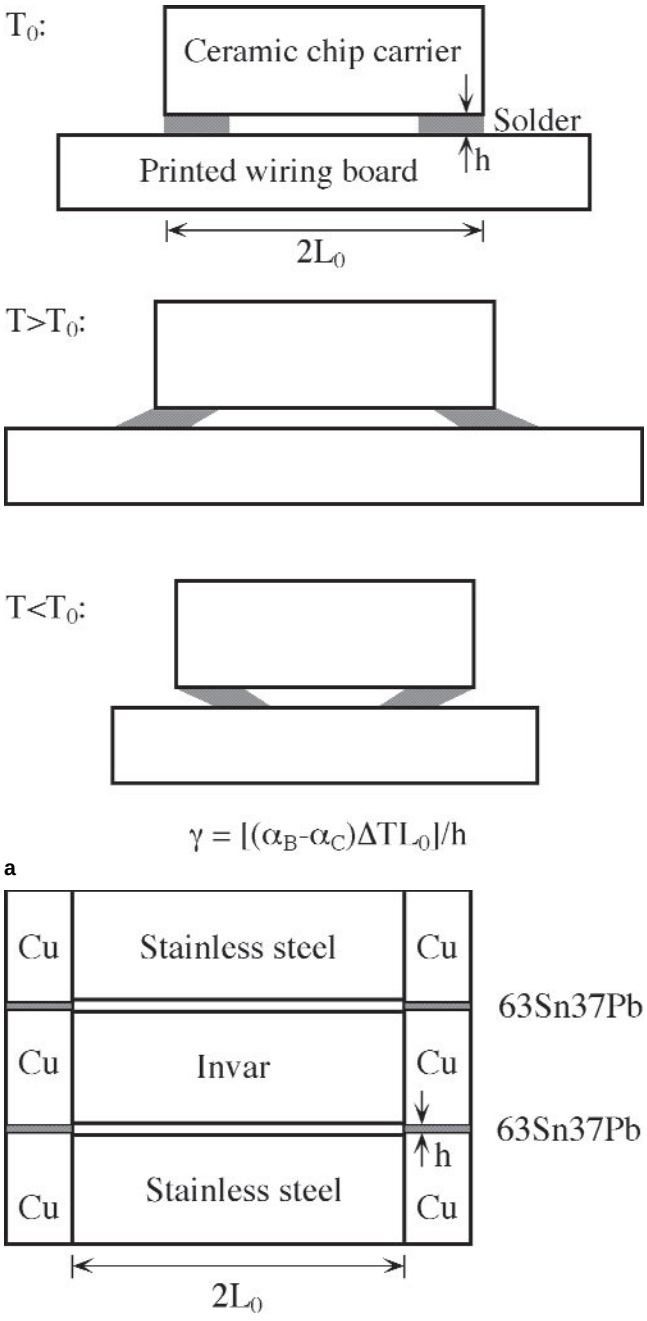

Fig. 1. (a) The schematic of the origin of shear strain, γ, caused by the mismatch between the thermal-expansion coefficients of the chip carrier, α_C, and the printed wiring board, α_B, when there is a temperature change of ΔT. (b) Testing assembly consisting of a loading frame and four solder joints.

of the strain levels is difficult, and testing under controlled conditions to develop constitutive equations for design and life prediction is impossible. A compromise is to use model joints that are sufficiently large to enable strain and stress measurement. The authors have used such a model joint that enables strain-controlled shear cycling to simulate the thermomechanical shear deformation experienced by solder joints, and have determined fatigue life as a function of plastic shear-strain range and hysteresis-loop energy.[17] In the present study, the resulting damage and microstructural changes produced in those experiments are reported.

EXPERIMENTAL DETAILS

Details of the equipment and methodology used in this study have been described previously.[17] Figure 1b shows the model joint and loading frame, which represent the component and substrate in an electronic package. The specimen comprises two stainless-steel bars surrounding a central Invar bar. The solder joint is formed between two copper blocks (6 mm $\times$ 10 mm $\times$ 12 mm) located at the end of the bars. The difference in thermal-expansion coefficient between stainless steel and Invar was measured to be 16.523×10^{-6} K^{-1} [17] and, because of this difference, the solder undergoes shear deformation during thermal cycling. Shear-strain ranges, from 0.0075–0.15, could be generated in the solder by altering the length of the loading bars and the thickness of solder layer. Joint dimensions, 10 $\times$ 6 $\times$ h mm (h varied between 0.25 mm and 2 mm, giving solder volumes between 15 mm^3 and 120 mm^3) were investigated. The symmetrical design eliminated bending of the frame.

The solder used was commercial-grade eutectic Sn-37Pb. To make a joint, the solder paste together with the copper blocks were preheated at 150°C for 10 min, followed by reflow soldering at 250°C for 10 min. The specimen was then directly quenched in cold water and stored in a freezer at −20°C. It was held at room temperature for about 15 h and polished using 0.05-μm alumina prior to testing. Some joints were sectioned through their center for microstructure observation, which was performed in a scanning electron microscope (SEM).

Temperature cycling was performed in air. The temperature profile consisted of a 1-h ramp up from room temperature to 125°C and a 1-h cooling to 30°C, with no dwell at the extremes. Subsequent cycles were between these temperature limits.

RESULTS

Macroscopic Deformation

The extent of macroscopic shear deformation was determined from the displacement of grinding lines intentionally left on the specimen surface prior to thermomechanical cycling. Figure 2a–c show these prior to the test, after 100 cycles under a strain range of 0.037 and after 30 cycles under a strain range of 0.09, respectively. The grinding lines adjacent to the copper substrate become curved, while those in the central area of the solder remain straight. High curvature indicates heavily deformed regions, or shear bands. These exist symmetrically adjacent to both interfaces between the solder and the intermetallic layer, and their curvature indicates the local distribution of deformation. Development of this curvature is incremental with cycles

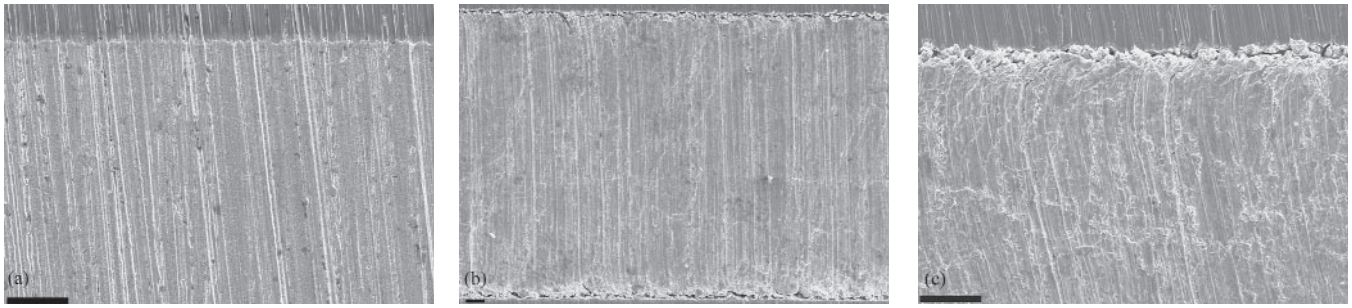

Fig. 2. The surface-grinding lines showing shear deformation produced by thermomechanical cycling: (a) initial condition, (b) after 100 cycles under a strain range of 0.037, and (c) after 30 cycles under a strain range of 0.09. Bar = 50 μm.

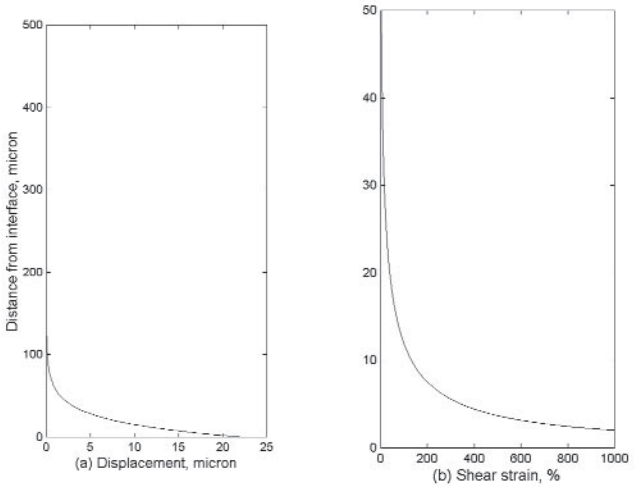

Fig. 3. (a) The displacement of the solder in a 1-mm-high joint subjected to thermomechanical cycling and (b) shear strain in the solder as a function of the distance from the interface.

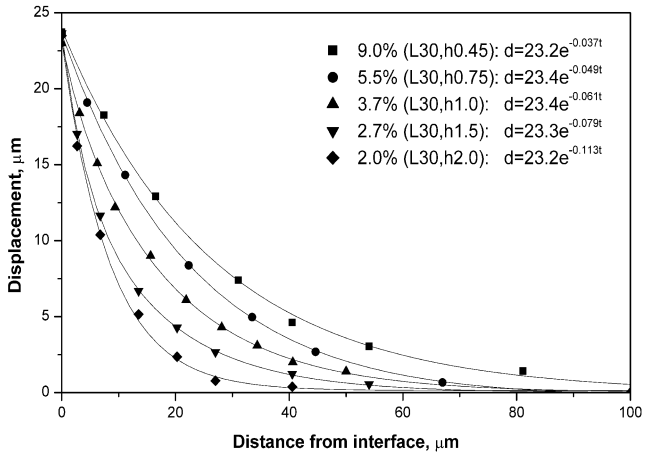

Fig. 4. The displacement of the solder in different model joints as a function of distance from the interface (L: length of the loading bar, mm; h: height of solder joint, mm).

but reaches a saturation level, and it is these values that are employed in their analysis. Figure 3a shows the shear displacement, d, obtained by digitizing the grinding lines, to be an exponential function of the distance, t, from the interface ($0 \leq t \leq 1/2$ h where h is the height of the solder joint).

$$d = d_0 e^{-\beta t} \quad (1)$$

where d_0 is the maximum displacement caused by thermomechanical cycling,[15] and β a factor between 0.04 and 0.11 for the joints tested.

Significant shear displacement occurred within a very narrow region (~50 μm) of the solder, adjacent and parallel to the interface. The magnitude of the shear strain decreases exponentially with the distance from the interface (Fig. 3b). The shear-strain levels at 50 μm, 20 μm, and 5 μm away from the interface are 3%, 40%, and 350%, respectively.

Figure 4 shows that, irrespective of joint geometry and strain range, the majority of displacement is concentrated in the solder within a 50-μm-wide region along the interface.

Cracking

Unlike conventional fatigue of bulk metals, crack initiation is rapid and may occur within the first cycle (Fig. 5). Cracking occurs primarily along the boundaries between the Sn-rich and Pb-rich phases, and mainly adjacent to the interface with the intermetallic layer (Fig. 5b). Some cracks also initiated along the actual interface between the solder and the intermetallic layer, as shown in Fig. 6. However, they constituted a small proportion of the interface length. These cracks occurred on the free surface (outer face) of the solder joint, but occasionally, they also initiated internally (Fig. 7). They are located on the Pb-rich and Sn-rich phases, as well as the interface between them, as indicated.

Cracking intensified with increasing strain range (Fig. 8). At the lower strain ranges, cracks appear as single lines lying adjacent to the interface (Fig. 8a and b), but with increasing strain range, multiple initiation occurs, and the damage band thickens (Fig. 8c and d). With continued cycling, damage caused by cracking accumulates (Fig. 9) and eventually results in the formation of a macrocrack.

At high shear-strain ranges, the grains of the solder are heavily deformed in the first cycle (Fig. 10a) and, with increasing cycles, fragmentation and macrovoiding occurs, as shown in Fig. 10b. Further agglomeration of the damage results in complete separation (Fig. 10c). However, at failure (defined in the associated endurance study as a 50% stress-

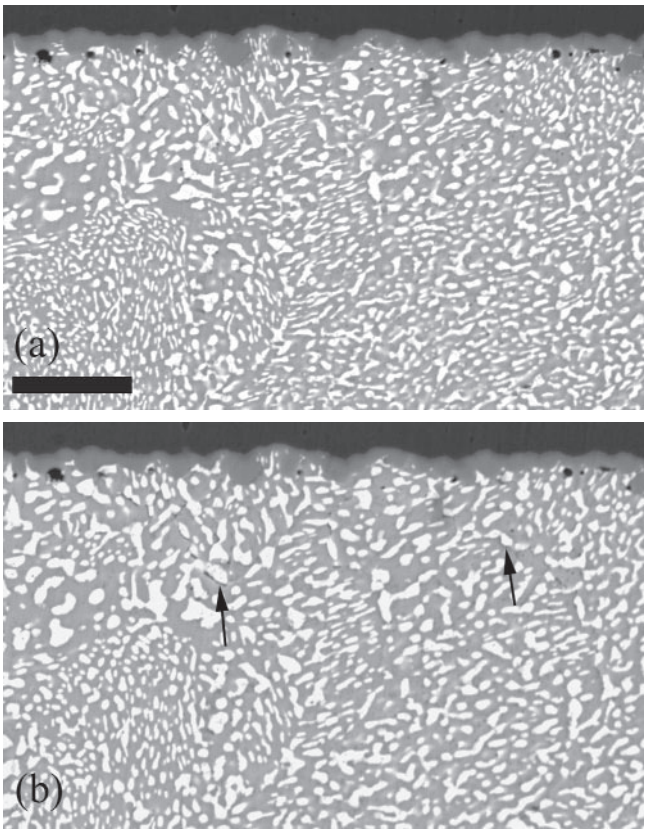

Fig. 5. The SEM backscattering images of crack initiation during thermomechanical cycling with a strain range of 0.0075: (a) initial condition and (b) after 1 cycle. Bar = 10 μm.

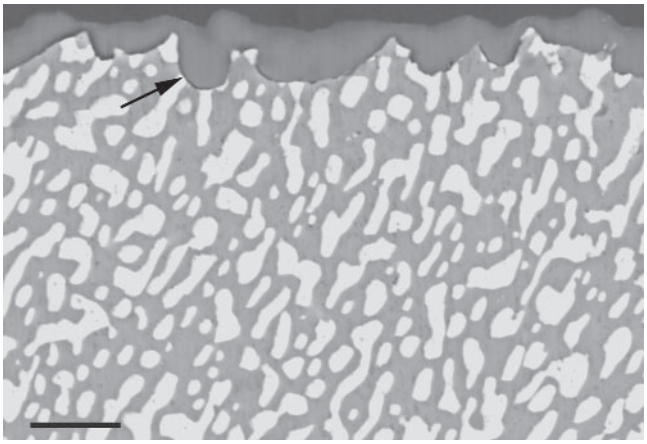

Fig. 6. The crack initiation (arrowed) along the interface in a solder joint after 1 cycle with a strain range of 0.0075. Bar = 5 μm.

range reduction), the extent of cracking on the surface is similar at all strain ranges. At this stage, local decohesion occurs, and a macrocrack extends from the edge into the interior solder, parallel to the shear deformation (Fig. 11). Those cracks initiating along the interface also produced local separation as they developed, as shown in Fig. 12.

In addition to the major cracking parallel to the interface, secondary cracks initiated from those cracks and grew on both the parallel and transverse faces

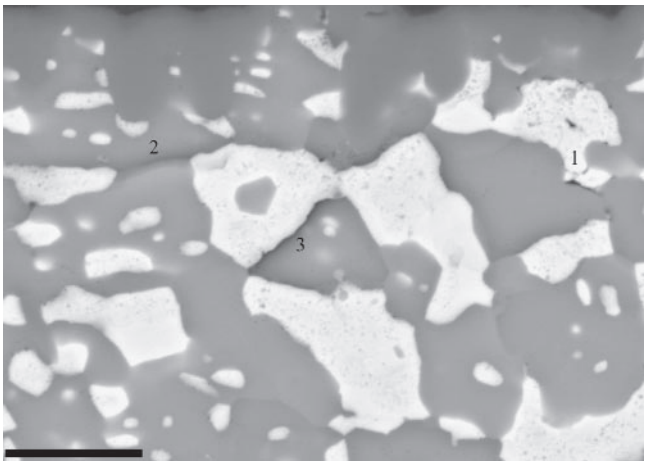

Fig. 7. The crack initiation in the interior of a solder joint that was sectioned along its mid section after 3 cycles with a strain range of 0.027: in Pb-rich phase, 1; in Sn-rich phase, 2; and in the boundaries between Pb-rich and Sn-rich phases, 3. Bar = 5 μm.

toward the interior of the solder, normal to the interface (Fig. 10). Figure 13 compares these two types of crack. The solder joint shown in Fig. 13a was repolished after thermomechanical cycling. While some cracks propagated along the phase boundaries, others penetrated Pb-rich or Sn-rich phases (grains), causing fragmentation. Figure 13b shows the secondary cracking along the colony boundaries on the surface of the solder. Within colonies, fine cracks propagate through the Sn-rich phase or along the phase boundaries between the Pb and Sn-rich phases. Distortion of the grinding lines in Fig. 14 shows that the deformation of the solder associated with secondary cracks involved the rotation of grains.

The secondary, vertical cracks are essentially surface cracks because their depth into the interior solder is very limited (Fig. 15), and they can be removed by repolishing (Fig. 16). Cracking was never observed at the intermetallic layer/copper interface.

To investigate the possible effect of initial surface finish, a solder joint, having both polished and as-cast regions on one of its surfaces, was examined. Figure 17 demonstrates the similarity of cracking in both areas and the absence of a discontinuity across the interface between them.

Microstructural Coarsening

The as-cast microstructure depends on the rate of cooling. Rapid solidification, which is more representative of actual joint history, produces a fine-grained globular structure of Pb-rich particles dispersed in the Sn-rich phase, as shown in Fig. 18. The average size of the Pb-rich phase is 0.6 μm. This microstructure is thermodynamically unstable and coarsens on exposure to most temperatures of interest, even below ambient. Figure 19a shows purely thermally induced coarsening after 250 thermal cycles between 30°C and 125°C (the size of the Pb-rich phase is 1.5 μm) in the absence of externally applied, cyclic strain. Hence, the microstructure can be taken as a

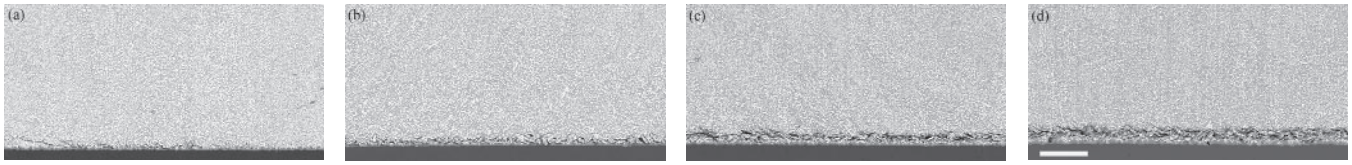

Fig. 8. The cracks formed after 1 cycle under the strain ranges of (a) 0.014, (b) 0.027, (c) 0.055, and (d) 0.09. Bar = 50 μm.

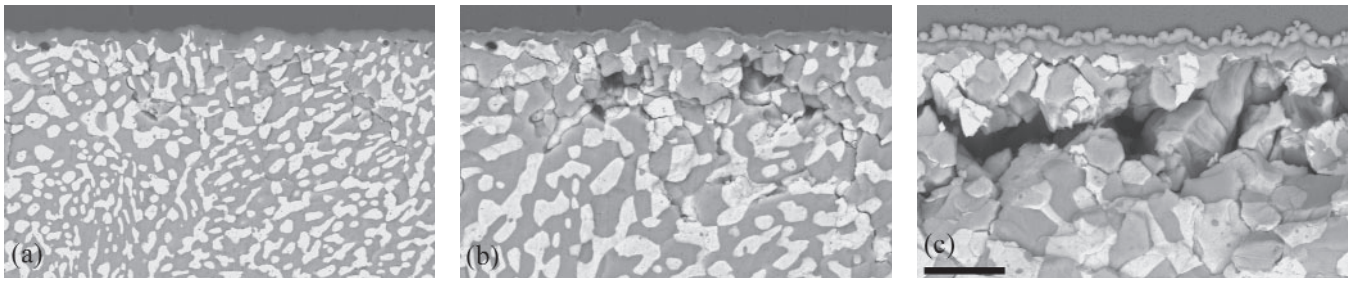

Fig. 9. The development of cracking with fatigue cycles under a strain range of 0.0075: (a) 10 cycles, (b) 100 cycles, and (c) 1,000 cycles. Figure 5 shows the initial and first cycle condition. Bar = 10 μm.

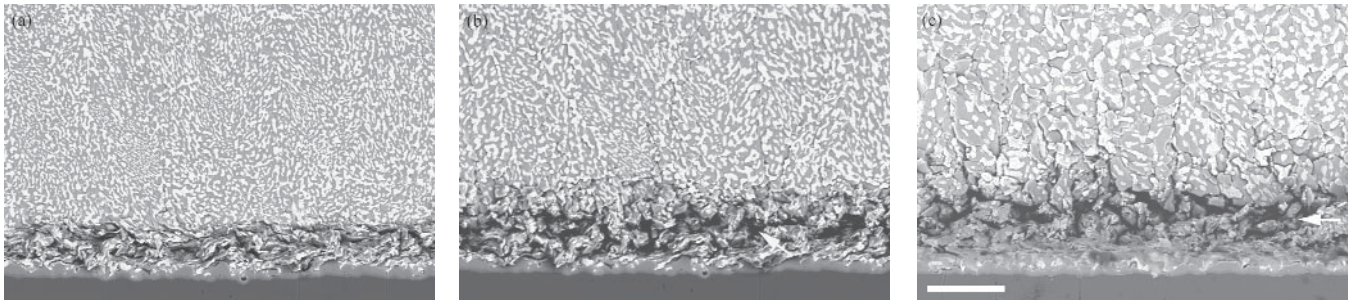

Fig. 10. The cracking under a strain range of 0.09 after (a) 1 cycle, (b) 5 cycles (holes indicated by arrow), and (c) 30 cycles (separation indicated by arrow). Secondary cracks present in (b) and (c) extending toward the center of the solder. Bar = 25 μm.

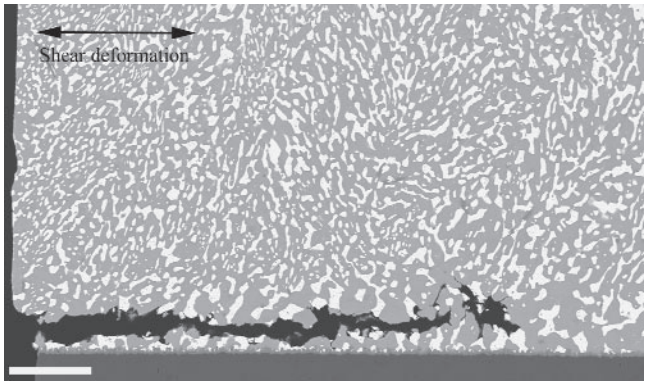

Fig. 11. The cracking in the direction parallel to shear deformation, sectioned after 275 cycles under a strain range of 0.027. Bar = 50 μm.

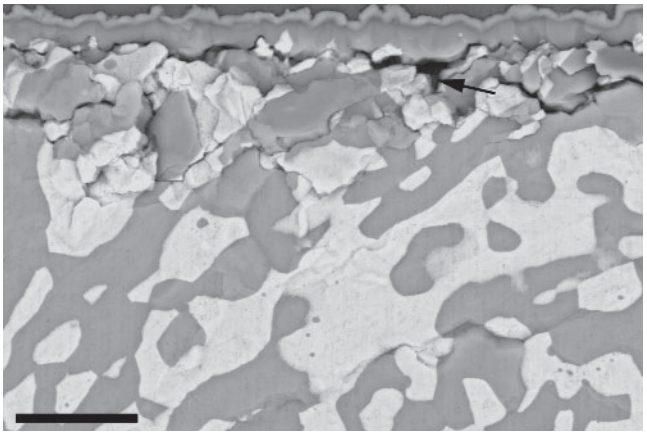

Fig. 12. The cracks along the solder/intermetallic interface after 300 cycles under a strain range of 0.0075. The separation of the solder from the interface is identified by an arrow. Bar = 10 μm.

reference base for the coarsening produced by both thermal and mechanical effects. Pure thermal cycling results in internal cracking. These are neglected in the present context.

Figures 19b and c show the coarsening after 250 cycles in a model joint tested under a strain range of 0.037. Coarsening varied according to location. In the central area of the solder, Fig. 19b, the size of the Pb-rich phase is 2.2 μm, slightly larger than that shown in Fig. 19a. However, adjacent to the interface, significant coarsening has occurred, and the Pb-rich phase size is 7 μm, more than three times larger than that in the central area (Fig. 19c).

Figure 20 compares the coarsening in the central area and along the interface in different specimens.

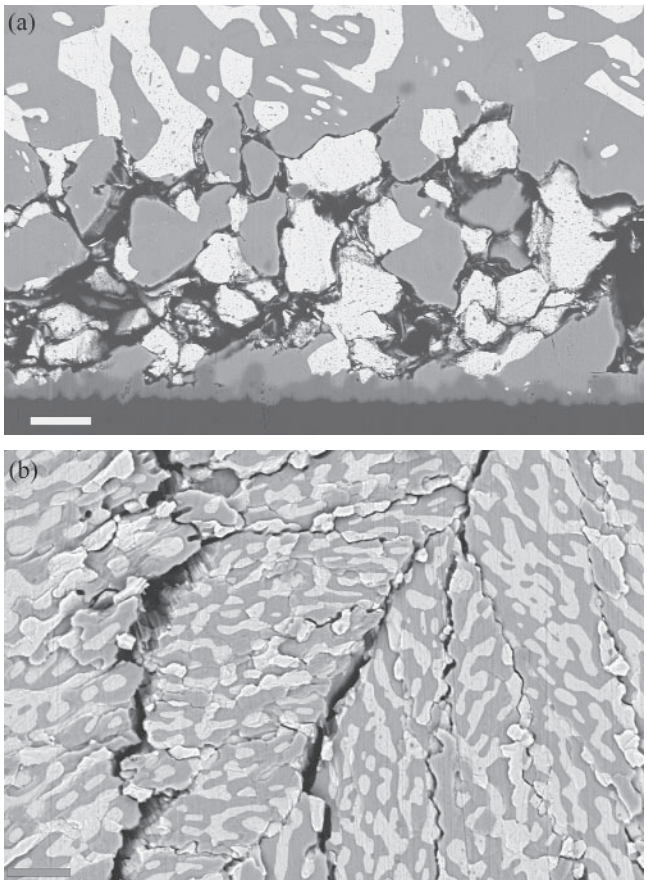

Fig. 13. The crack types caused by thermomechanical cycling: (a) primary cracks adjacent to the interface in a joint repolished after 1,000 cycles under a strain range of 0.02 and (b) secondary cracks in the central surface after 250 cycles under a strain range of 0.027. Bar = 10 μm.

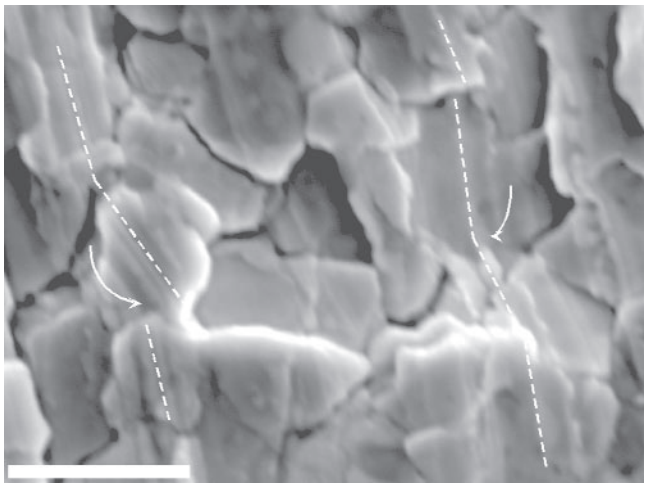

Fig. 14. The rotation of grains associated with secondary cracks revealed by distortion of grinding lines. Bar = 2 μm.

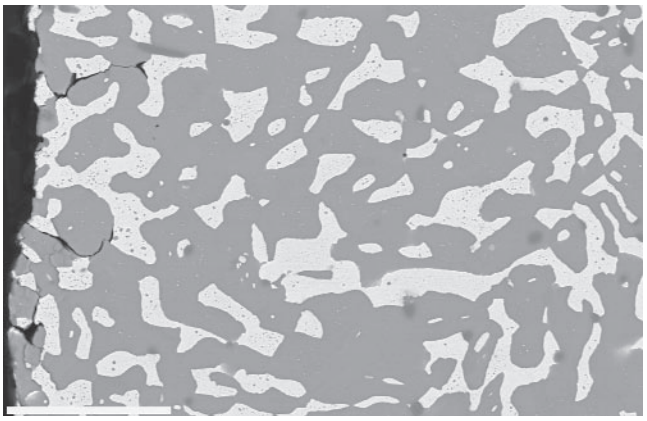

Fig. 15. The depth of secondary cracks in a solder joint sectioned after 1,770 cycles under a strain range of 0.014. Bar = 50 μm.

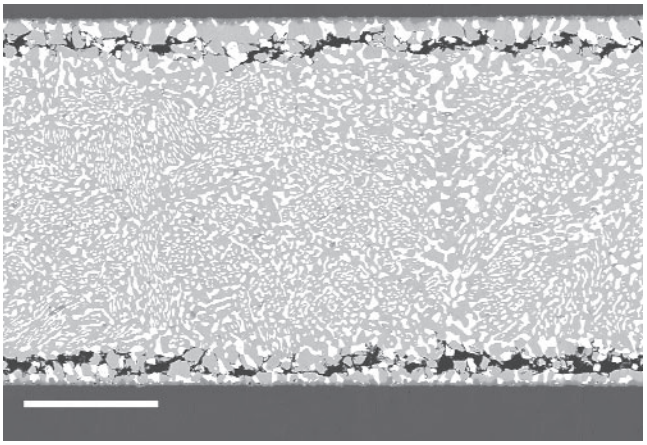

Fig. 16. The SEM backscattering image of cracks in a solder joint repolished after 30 cycles under a strain range of 0.15. Bar = 100 μm.

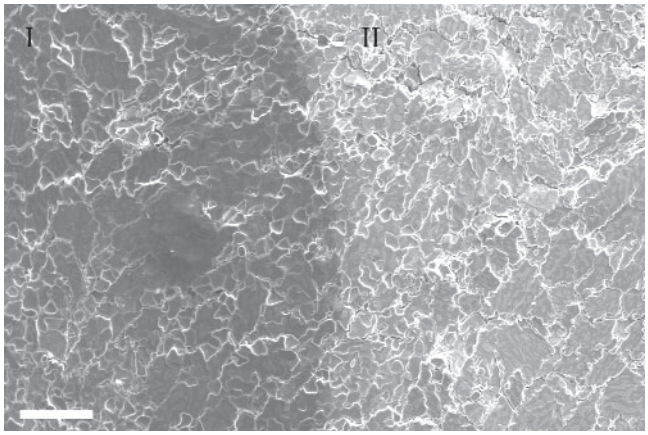

Fig. 17. The cracks on as-cast (I) and polished (II) areas in a solder joint after 100 cycles under a strain range of 0.027. Bar = 100 μm.

For the model joints subjected to thermomechanical cycling, the coarsening occurring in the central area is the same as that in the specimen that experienced temperature cycling, indicating that the coarsening in this area is basically thermally induced. As discussed earlier, strain is concentrated along the interface. In the area with strain concentration, significant coarsening occurred, although it appears insensitive to strain range.

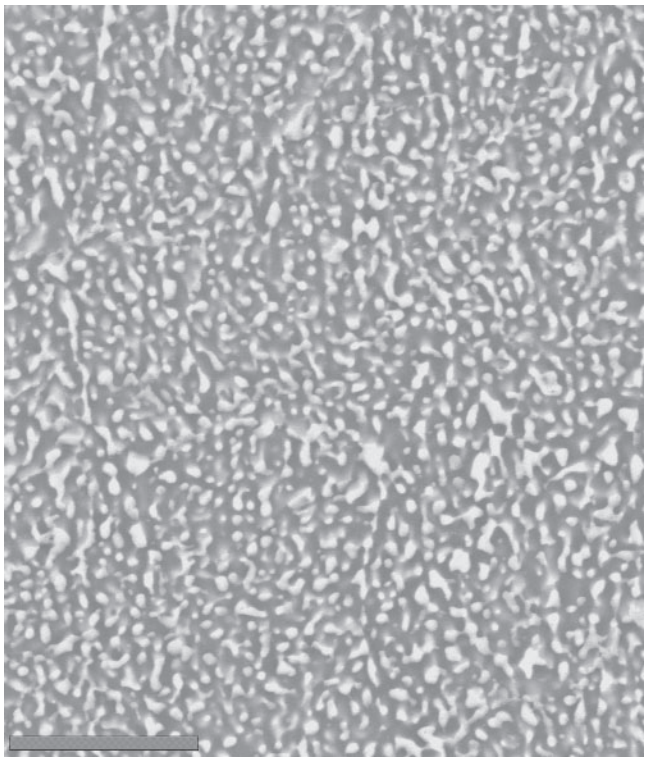

Fig. 18. The microstructure of 63Sn37Pb obtained by water quenching. Bar = 10 μm.

Longitudinal sectioning through the center of the joint indicates that all the cracks are removed, but coarsening remains (Fig. 21), suggesting that coarsening is a precursor to cracking in these regions.

Intermetallic Layer

Figure 22 shows the intermetallic layer, i.e., Cu_6Sn_5, before and after thermomechanical cycling. The layer thickness is 3 μm on average, and its upper surface undulates quite significantly. After thermomechanical cycling, the layer consolidates rather than increases its overall thickness by further penetration into the solder (Fig. 22b and c). The intermetallic layer itself shows little evidence of damage. Only occasionally were cracks found in the intermetallic layer. They were contained within it and are unlikely to have contributed to the deterioration of the solder joint, although it is not clear when and how they occurred.

DISCUSSION

When Sn-37Pb model-solder joints are subjected to cyclic shear deformation during thermomechanical cycling, the changes induced are strongly location sensitive. The development of shear bands in the solder adjacent to the interface between the solder and the intermetallic compound accommodates

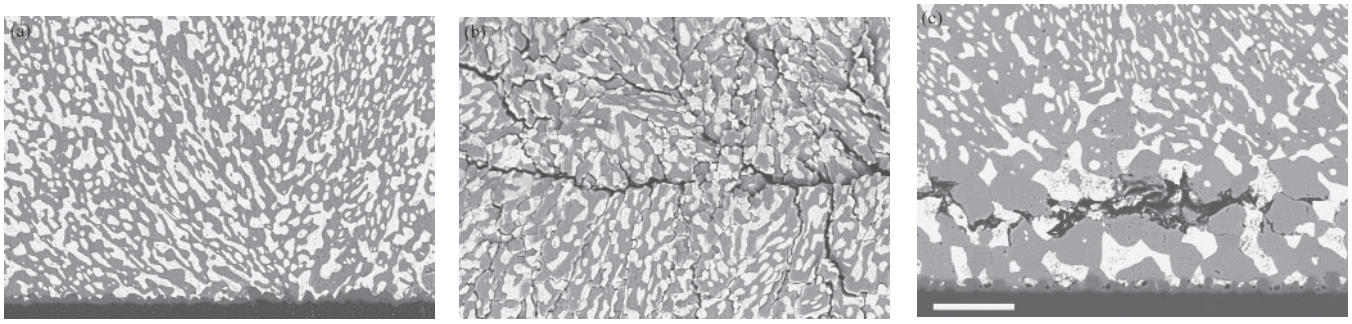

Fig. 19. The microstructural coarsening after 250 thermal cycles (a) between 30–125°C without external strain, (b) at the central surface area tested under a strain range of 0.037, and (c) at the area along the interface after repolishing. Bar = 25 μm.

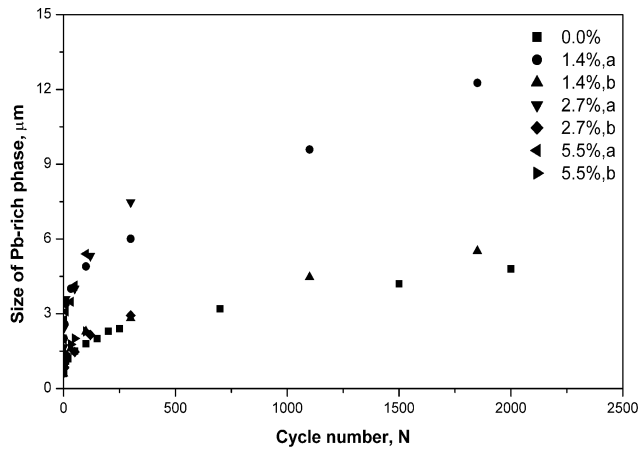

Fig. 20. The microstructural coarsening in the model joints with different strain ranges: (a) at strain concentration area and (b) at central area.

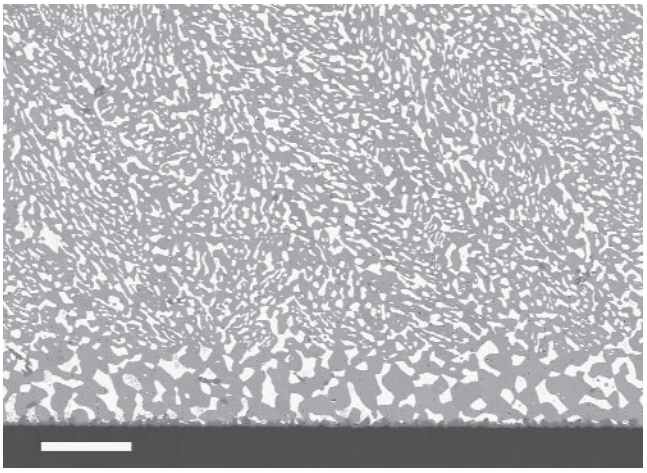

Fig. 21. The internal coarsening at the mid section of the joint shown in Fig. 19b and c. Bar = 50 μm.

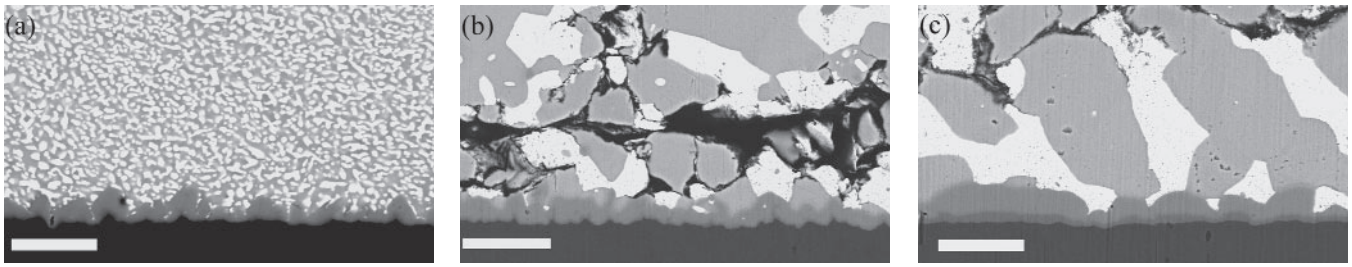

Fig. 22. The intermetallic layer: (a) initial state, (b) after 1,000 cycles under a strain range of 0.014, and (c) after 300 cycles under a strain range of 0.09. Bar = 10 μm.

the majority of the deformation. The severity of deformation diminishes exponentially with distance from the interface and is essentially zero at the mid-thickness regions.

The formation of shear bands is a common consequence of mechanical- and thermal-cyclic deformation, particularly in alloys that exhibit cyclic softening. In such cases, the softened regions act as easy paths for subsequent deformation. Many bulk solder alloys, including Sn-37Pb, fall into this category. It has been proposed[8] that the irregular coarsening of eutectic SnPb may be due to an increase in short-circuiting diffusion paths produced by the plastic deformation of the phases or dynamic recrystallization that occurred during thermomechanical cycling. An irregularly coarsened band is weaker than the rest of the solder, and the imposed strain concentrates in this region. The location of cracks slightly away from the solder/intermetallic interface is a common, but not fully explained, phenomenon.[10,18] As with laminates, the bond quality is likely to govern the strengthening effect into the softer material.

Cracking occurs rapidly in the shear bands, often after the first cycle at phase boundaries. With further cycling, multiple initiation, phase fragmentation, and decohesion occur, forming a gross macrocrack, aligned in the direction of shear. This crack also penetrates into the interior of the solder. Concomitantly, microstructural coarsening takes place and is significantly enhanced by the high cyclic strains in the shear bands. In addition, secondary cracks are developed from the major crack and propagate in the surface layers along colony boundaries approximately perpendicular to the main crack plane. As-cast and polished surfaces exhibit similar characteristics.

These two types of cracks involve different mechanisms. The cracks in the shear band, i.e., in the high-strain area, are transgranularly dominant, while the secondary cracks in the low-strain area are intergranular. These two mechanisms are cooperative, resulting in the coexistence of two types of cracks in a joint. However, they have a different significance for the endurance of the solder joints. Those within the shear bands initiate first and propagate in the region adjacent to the interface through the entire joint. In contrast, the secondary cracks propagate along colony boundaries, but they are limited to the outer surface layers and have little impact on fatigue life.

The observation of immediate cracking in some cases suggests that both cracking and softening contribute to the stress-range drop observed during thermomechanical cycling of the joint. However, within the interior of the solder, there was evidence that coarsening was a precursor to cracking. Most definitions of fatigue failure involve a stress-drop parameter, and in bulk materials, this is assumed to be the result of deformation-induced changes in strength together with the initiation of a single predominant crack. If, as seems likely from the present study, the measured stress changes are more influenced by cracking, then greater care will be required in comparing data from different sources, as pointed out by Frear.[19]

The fact that shear bands develop only in the region adjacent to the interface might be related to the nature of the interface. In general, when two materials with different crystal structures are coupled together, the region around the interface becomes a source for crystal defects and facilitates subsequent deformation.[20] However, because the shear strain, γ, is

$$\gamma = \frac{d}{t} = \frac{d_0 e^{-Bt}}{t} \tag{2}$$

the solder very close to the interface experiences strains too large to be accommodated and cracking occurs. This might explain why the cracks are generally formed a distance away from the interface.

Given the three-dimensional nature of the model joint, the cracking mechanisms are quite complex. Most observations were taken of the front vertical face of the joint, parallel to the shear direction (the parallel face). Within this plane, individual cracks developed by a combination of Mode I and Mode II opening, but penetration into the interior of the solder involves a Mode III opening component. Mode I opening involves vertical separation of the crack faces within the plane of the specimen; Mode II opening involves parallel shearing of the faces within this plane; whereas in Mode III opening, out-of-plane shearing, similar to tearing, occurs. Crack growth from the vertical face, perpendicular to this and the shear direction (the transverse face), involves Mode I and Mode II opening. Multiple initia-

tion, linkage, and fragmentation results in the coarse-macroscopic cracks observed, although at this more global level, the opening modes are similar to those described. The secondary cracks visible on the parallel and transverse faces extend primarily by Mode I opening with a limited Mode III component, as evidenced by their disappearance after removal of the surface layers by polishing. Further work is underway to gauge the three-dimensional crack profile, and this will be reported subsequently, together with the crack-growth data. The situation described does indicate the magnitude of the challenge facing life-prediction approaches that are based upon crack-growth parameters.

The intermetallic layer does not decay during thermomechanical cycling even when the solder adjacent to it has been ruptured. No connection has been found between intermetallic layer and the cracks or microstructural changes occurring in the solder. Therefore, it appears that the intermetallic layer is not involved in the fatigue process in a solder joint, and its significance is indirect, arising from its role as an interface.

SUMMARY AND CONCLUSIONS

Thermomechanical cycling tests were performed on the 63Sn37Pb solder-model joints over a temperature range from 30°C to 125°C with a cycle period of 2 h. The formation of shear bands, primary and secondary cracks, heterogeneous and irregular coarsening of Sn-37Pb, consolidation of intermetallic layer, and cracks on intermetallic layer were observed. The following conclusions provide more detail.

- A strain concentration zone, i.e., shear band, is formed along the interface between the Sn-37Pb and the intermetallic layer, and the shear strain increases exponentially with proximity to the interface.
- Cracks initiate mainly on the free outer surface of the solder and propagate transgranularly toward the interior regions of the joints within the shear bands. The development of these cracks determines the lifetime of the joints. Secondary cracks grow intergranularly within surface layers and are unlikely to affect the reliability.
- Heterogeneous microstructural coarsening occurs throughout the joints, and irregular coarsening occurs within the shear bands. Coarsening precedes cracking.
- The intermetallic layer is largely unaffected, although valleys at the solder interface tend to fill out.

ACKNOWLEDGEMENTS

This research was supported by EPSRC. The authors express thanks to Professor Adrian Hopgood for his comments on interfacial structure of materials and to C. Gagg, J. Moffatt, N. Williams, and S. Hiller for their technical support.

REFERENCES

1. S.K. Kang and A.K. Sarkhel, *J. Electron. Mater.* 23, 701 (1994).
2. K.C. Liu and J.G. Duh, *IEEE Trans. Comp. Hybrids Manuf. Technol.* 14, 703 (1991).
3. J. Lynch and A. Boetti, *Thermal Stress and Strain in Microelectronics Packaging*, ed. J.H. Lau (New York: Van Nostrand Reinhold, 1994), pp. 579–606.
4. J.H. Lau and Y.H. Pao, *Solder Joint Reliability of BGA, CSP, Flip, Chip, and Fine Pitch SMT Assemblies* (New York: McGraw-Hill, 1997), pp. 153–218.
5. R.N. Wild, *Welding Res. Suppl.* 51, 521s (1972).
6. J.T. Lynch, M.R. Ford, and A. Boetti, *IEEE Trans. Comp. Hybrids Manuf. Technol.* 6, 237 (1983).
7. D. Frear, *IEEE Trans. Comp. Hybrids Manuf. Technol.* 12, 492 (1989).
8. P. Hacke, A.F. Sprecher, and H. Conrad, *ASME J. Electron. Packag.* 115, 153 (1993).
9. J.W. Morris, Jr., J.L. Freer Goldstein, and Z. Mei, *The Mechanics of Solder Alloy Interconnections*, ed. D. Frear, H. Morgan, S. Burchett, and J. Lau (New York: Van Nostrand Reinhold, 1994), pp. 7–41.
10. Z. Guo and H. Conrad, *ASME J. Electron. Packag.* 115, 159 (1993).
11. J.L. Marshall, L.A. Foster, and J.A. Sees, *The Mechanics of Solder Alloy Interconnections*, ed. D. Frear, H. Morgan, S. Burchett, and J. Lau (New York: Van Nostrand Reinhold, 1994), pp. 42–60.
12. K. Jung and H. Conrad, *J. Electron. Mater.* 30, 1294 (2001).
13. H.L.J. Pang, K.H. Tan, X.Q. Shi, and Z.P. Wang, *Mater. Sci. Eng.* A307, 42 (2001).
14. D. Frear, D. Grivas, and J.W. Morris, Jr., *J. Electron. Mater.* 17, 171 (1988).
15. H.D. Solomon, *Low-Frequency, High-Temperature Low Cycle Fatigue of 60Sn-40Pb Solder*, ASTM STP 942 (Philadelphia, PA: ASTM, 1988).
16. P.M. Hall, T.D. Dudderar, and J.F. Argyle, *IEEE Trans. Comp. Hybrids Manuf. Technol.* 6, 544 (1983).
17. X.W. Liu and W.J. Plumbridge, "Fatigue of Sn-37Pb Solder Joints under Thermomechanical Cycling," in preparation for publication.
18. A.R. Syed, *J. Electron. Packag.* 117, 116 (1995).
19. D.R. Frear, *IEEE Trans. Comp. Hybrids Manuf. Technol.* 12, 492 (1983).
20. X.W. Liu, (Ph.D. thesis, The Open University, England, 1999).